






## Excitation spectra of the heaviest carbon isotopes investigated within the CD-Bonn Gamow shell model

Y. F. Geng <sup>1</sup>, J. G. Li,<sup>1</sup> Y. Z. Ma,<sup>1</sup> B. S. Hu <sup>1</sup>, Q. Wu,<sup>1</sup> Z. H. Sun <sup>2</sup>, S. Zhang <sup>1</sup> and F. R. Xu <sup>1,\*</sup>

<sup>1</sup>*School of Physics, and State Key Laboratory of Nuclear Physics and Technology, Peking University, Beijing 100871, China*

<sup>2</sup>*Physics Division, Oak Ridge National Laboratory, Oak Ridge, Tennessee 37831, USA*



(Received 19 May 2022; revised 14 July 2022; accepted 27 July 2022; published 3 August 2022)

Neutron-rich carbon isotopes have been investigated within the Gamow shell model (GSM) based on a realistic nuclear force.  $^{14}\text{C}$  was chosen as the core in the shell-model calculations of the neutron-rich carbon isotopes. The effect from the coupling to the continuum is well considered by using the complex-momentum Berggren representation which treats bound, resonant, and continuum states on an equal footing. Using the many-body perturbation theory named the  $\hat{Q}$ -box folded-diagram method, the complex GSM effective interaction was derived from the CD-Bonn interaction. We find that the inclusion of the continuum coupling in the calculation is important in the description of neutron-rich carbon isotopes, especially in reproducing the experimental  $1/2^+$  ground states of  $^{19}\text{C}$  and  $^{21}\text{C}$ . Our calculation indicates a shell closure at  $N = 16$  in the carbon chain, while the  $N = 14$  shell, which exists in the next even- $Z$  chain of oxygen isotopes, disappears. The calculation suggests that  $^{22}\text{C}$  is the heaviest bound carbon isotope, i.e., the neutron drip line.

DOI: [10.1103/PhysRevC.106.024304](https://doi.org/10.1103/PhysRevC.106.024304)

### I. INTRODUCTION

Neutron-rich carbon isotopes provide an intriguing laboratory for the studies of intricate effects in the exotic nuclei of drip line regions, e.g., nuclear forces and continuum effect. Compared with the next even- $Z$  chain of oxygen isotopes, the carbon chain has more isotopes with halo structure observed experimentally, such as  $^{15}\text{C}$  [1–3],  $^{19}\text{C}$  [3–6], and  $^{22}\text{C}$  [7,8]; and the  $N = 14$  neutron shell [9,10], which exists in the oxygen chain [11,12], disappears. Experiments have provided rich and interesting data on carbon excited states with particle-unstable resonances observed [13–16] which are still challenging theoretical calculations.

$^{19}\text{C}$  is the last bound odd- $A$  carbon isotope with a small one-neutron separation energy. Shell models with phenomenological interactions such as WBP [16–18], WBT [16], YSOX [18], and SFO [16,18,19] have been applied to carbon isotopes. However, the calculations cannot well describe the excitation spectra of odd- $A$  carbon isotopes. In  $^{19}\text{C}$ , for instance, only the SFO interaction can reproduce the correct order of the levels [18]. Calculations based on realistic nuclear forces have also been performed for carbon nuclei, e.g., the realistic-interaction shell model (RSM) [20], coupled-cluster effective interaction (CCEI) [17], and valence-space in-medium similarity renormalization group (VS-IMSRG) [21]. The CCEI calculations [17] cannot reproduce the experimental  $1/2^+$  ground states of  $^{19,21}\text{C}$ , while no  $J^\pi$  information had been provided in the literature of the VS-IMSRG calculations [21]. We found that all the calculations mentioned above did not consider the continuum effect, which can be significant

in weakly bound nuclei. In contrast to the isotone  $^{21}\text{O}$  in which the  $0d_{5/2}$  orbital is occupied, the last neutron in the weakly bound  $^{19}\text{C}$  fills the  $1s_{1/2}$  orbital. The neutron  $1s_{1/2}$  orbital, which is a weakly bound level in neutron-rich carbon isotopes, plays an important role in the formation of the one-neutron halo in  $^{19}\text{C}$  [4,22,23]. It was commented that the continuum effect should be important in reproducing the low-lying states of  $^{19}\text{C}$  [16,17]. The complicated coupling to the continuum states in neutron-rich carbon isotopes remains a challenge to current theoretical calculations. In the present work, one of our main motivations is to investigate the continuum effect in the ground states and low-lying excited states of neutron-rich carbon isotopes.

The continuum effect was considered in the important-truncated no-core shell model with continuum (IT-NCSMC) [24] in which  $^{17}\text{C}$  was calculated, showing that the lowest  $1/2^+$  state becomes more bound due to the continuum coupling. However, the IT-NCSMC calculation in Ref. [24] can only handle a basis size up to  $N_{\text{max}} = 6$ , which is insufficient for carbon isotopes. The Gamow IMSRG [25] was applied to the closed-shell  $^{22}\text{C}$ , showing the importance of the inclusion of the  $s$ -wave continuum in reproducing the extended halo density distribution. However, the Gamow IMSRG only works for closed-shell nuclei. In the present work, we investigate neutron-rich carbon isotopes with focus on the continuum effect.

The standard shell model using the harmonic oscillator (HO) basis cannot describe the continuum feature due to the strong locality of wave functions. In the present work, we choose the Gamow shell model (GSM) [26] with a realistic interaction used to investigate neutron-rich carbon isotopes. The continuum effect is taken into account by employing the Berggren basis [27] in which, by extending to the

\*frxu@pku.edu.cn

TABLE I. Neutron single-particle energies (in MeV) calculated by the WS potential, compared with data [33,34]. The resonance orbital  $0d_{3/2}$  is indicated by a complex energy of  $E - i\Gamma/2$  with  $\Gamma$  being the resonance width.

$nlj$	Calculated	Experimental
$0d_{3/2}$	$3.59 - i0.90$	$3.56 - i0.87$
$0d_{5/2}$	-0.47	-0.48
$1s_{1/2}$	-1.21	-1.22

complex-momentum plane, the bound, resonance, and continuum states are treated on an equal footing.

## II. OUTLINE OF GAMOW SHELL MODEL WITH A REALISTIC INTERACTION

The translationally invariant intrinsic Hamiltonian of the  $A$ -nucleon system used in this work reads [26,28]

$$H = \sum_{i=1}^A \left( 1 - \frac{1}{A} \right) \frac{\mathbf{p}_i^2}{2m} + \sum_{i<j}^A \left( V_{ij}^{\text{NN}} - \frac{\mathbf{p}_i \cdot \mathbf{p}_j}{mA} \right), \quad (1)$$

where  $\mathbf{p}_i$  is the nucleon momentum in the laboratory system and  $m$  is the nucleon mass.  $V_{ij}^{\text{NN}}$  is the nucleon-nucleon (NN) interaction. In the present work, we choose the CD-Bonn NN interaction [29]. As in the standard shell model, the  $A$ -body Hamiltonian is separated into a one-body part and a residual two-body part [26,28,30,31] as

$$H = \sum_{i=1}^A \left( \frac{\mathbf{p}_i^2}{2m} + U_i \right) + \sum_{i<j}^A \left( V_{ij}^{\text{NN}} - U_i - \frac{\mathbf{p}_i^2}{2Am} - \frac{\mathbf{p}_i \cdot \mathbf{p}_j}{Am} \right) = H_0 + H_1, \quad (2)$$

where  $H_0 = \sum_{i=1}^A \left( \frac{\mathbf{p}_i^2}{2m} + U_i \right)$  has a form of independent-particle motions in the one-body potential  $U_i$  for which we choose the Woods-Saxon (WS) potential.  $H_1$  is the residual two-body interaction with the correction from the center-of-mass (CoM) motion.

The closed-shell  $^{14}\text{C}$  is chosen as the inert core of the GSM calculation for neutron-rich carbon isotopes. The  $^{14}\text{C}$  WS potential is used to generate the Berggren basis [26], and mimics the one-body potential  $U_i$  produced by the core. The WS parameter values are determined by fitting experimental neutron single-particle energies of the  $^{14}\text{C} + n$  system, which are obtained in fact by the  $^{15}\text{C}$  data. If the single-particle state is unbound, the resonance width of the state also needs to be considered in the fitting. The chosen parameters are  $V_0 = 60.0$  MeV for the potential depth,  $V_{\text{so}} = 10.6$  MeV for the spin-orbital coupling strength,  $r_0 = 1.13$  fm for the radius parameter, and  $a = 0.60$  fm for the diffuseness. Table I summarizes the experimental and calculated neutron single-particle energies, in which the resonance width of the  $0d_{3/2}$  orbital is also reproduced. In fact, we mainly adjust the values of parameters  $V_0$  and  $V_{\text{so}}$ , while  $r_0 = 1.13$  fm and  $a = 0.60$  fm are around the common values used in WS nuclear structure calculations [32].

The Berggren completeness relation [27] covers bound, resonance, and continuum states, presented with a contour in a complex-momentum plane [26]. Continuum partial waves are discretized by the Gauss-Legendre quadrature method in practical computations [26,35–37]. The  $0d_{3/2}$  orbital is a resonance with a negative imaginary part of the energy, located in the fourth quadrant of the complex-momentum coordinate system [26]. For the  $d_{3/2}$  channel, the contour is chosen as  $L^+ = \{0 \rightarrow (4 - 2i) \rightarrow 8 \rightarrow 100\}$  (in MeV) to enclose the  $0d_{3/2}$  resonance. Each continuum contour is discretized with 34 discretization points. We have well tested that such discretization is sufficient to get a converged result [26,28,38–40]. The  $1s_{1/2}$  orbital is bound in neutron-rich  $sd$ -shell nuclei. There is no neutron  $s$ -wave resonance due to the absence of a centrifugal barrier. The inclusion of the  $s$ -wave continuum could be important in the description of loosely bound and resonance states in which the wave functions have large spatial spreads [25]. In the present calculations, the  $s_{1/2}$  continuum is included in the model space of valence particles, with the same contour chosen as for the  $d_{3/2}$  partial wave.

The realistic nuclear force has a strong short-range repulsive core, which makes the numerical calculation difficult. We renormalize the bare force using the  $V_{\text{low-}k}$  method [41] with a cutoff at  $\Lambda = 2.6$  fm $^{-1}$ , and the calculations of low-lying states are not sensitive to the cutoff [26]. The renormalized CD-Bonn interaction is first calculated in the laboratory HO basis using the Brody-Moshinsky brackets [42], and then converted to the Berggren basis by computing overlaps between the HO and Berggren basis wave functions [30]. With the  $^{14}\text{C}$  core, we choose neutron  $\{0d_{5/2}, 1s_{1/2}$  plus  $s$ -wave continuum,  $0d_{3/2}$  resonance plus  $d_{3/2}$ -wave continuum $\}$  as the GSM model space. We use the full  $\hat{Q}$ -box folded diagrams [30] to construct the realistic effective interaction for valence neutrons within the complex Berggren basis. The model space spanned with continuum partial waves is nondegenerate, and may break the order-by-order perturbation due to the vanished energy denominator. We use the extended Kuo-Krenciglowa (EKK) method [30,43] to derive the effective interaction. When the continuum is included, the dimension of the model is huge. Therefore, we calculate the  $\hat{Q}$ -box diagrams up to the second order of the perturbation. In the following GSM many-body calculation, we restrict to a maximum of two valence neutrons in the continuum. We have tested that the change in the excitation energy of a state is less than 1 keV if a third valence neutron is allowed in the continuum in the  $^{19}\text{C}$  GSM calculation. The complex-symmetric GSM Hamiltonian obtained thus is diagonalized in the model space specified above, using the  $m$ -scheme Jacobi-Davidson method [44,45].

## III. CALCULATIONS AND DISCUSSIONS

We have applied the CD-Bonn GSM to the heavy neutron-rich carbon isotopes. Figure 1 shows calculated excitation levels for  $^{19}\text{C}$ , compared with the data [14–16]. We see that the order of the  $^{19}\text{C}$  low-lying levels is reproduced by the CD-Bonn GSM calculation. To investigate the continuum effect, we have also performed a conventional SM calculation within a HO basis with the same  $V_{\text{low-}k}$  CD-Bonn interaction. The infinitely deep HO potential isolates the coupling to the

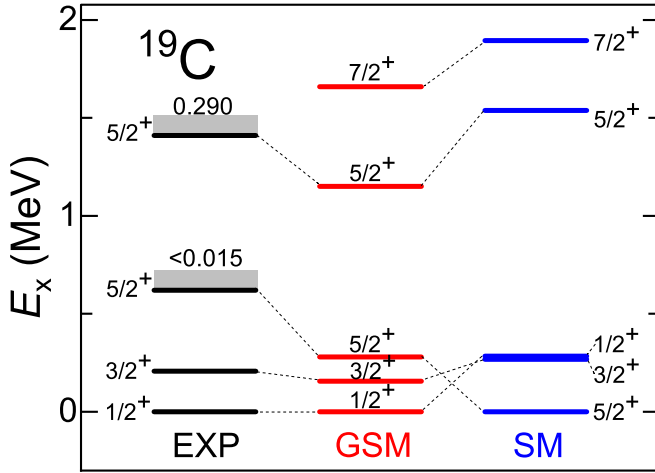


FIG. 1.  $^{19}\text{C}$  experimental [14–16] and calculated levels by the GSM and the real-energy SM (indicated by SM) using the same CD-Bonn interaction. The resonance state is marked by shadowing with the resonance width (in MeV) given above the level.

continuum. The SM Hamiltonian solved in the HO basis gives real-energy eigenvalues. We refer to this as the real-energy SM calculation to distinguish it from the complex-energy GSM calculation. In the real-energy SM, we take the model space  $v\{1s_{1/2}, 0d_{5/2}, 0d_{3/2}\}$ , similar to that in GSM, but without the continuum. The single-particle energies of the neutron  $1s_{1/2}$ ,  $0d_{5/2}$ , and  $0d_{3/2}$  orbitals are chosen to be the same as in the GSM. The same order of the  $\hat{Q}$ -box perturbation as in the GSM is used, i.e., up to the second order of the perturbation. In Fig. 1, we see that the real-energy SM calculation without the continuum effect gives a  $5/2^+$  configuration rather than the experimental  $1/2^+$  state for the ground state. By calculating the spectroscopic factor of the  $^{19}\text{C}$  ground state with respect to the  $^{18}\text{C} + n$  structure, we find that the lowest  $1/2^+$  state in the GSM calculation has a dominant configuration with the last neutron occupying the  $1s_{1/2}$  orbital, while the lowest  $5/2^+$  state in the real-energy SM calculation has a dominant component with the last neutron filling the  $0d_{5/2}$  orbital. The weakly bound  $1s_{1/2}$  neutron orbital with a zero centrifugal barrier ( $l = 0$ ) has a strong coupling to the continuum, which significantly lowers the energy of the  $1/2^+$  state, and leads to the correct  $1/2^+$  ground state in the GSM calculation. In Ref. [46], it has also been found that the neutron  $s$ -wave is important in determining the relative position between the  $1/2^+$  and  $5/2^+$  states in weakly bound light nuclei.

In the  $^{19}\text{C}$  experimental spectrum, the first  $5/2^+$  level at  $E_x = 0.62(9)$  MeV is slightly higher than the one-neutron emission threshold [ $S_n = 0.58(9)$  MeV] of the nucleus [16]. The experiment suggests a narrow resonance for this  $5/2^+$  state with an estimated resonance width of  $\Gamma < 0.015$  MeV [16]. The second  $5/2^+$  state has a resonance width of 0.29 MeV [14]. However, the present calculation does not give the resonance at low excitation energy in  $^{19}\text{C}$ . The calculated one-neutron separation energy is  $S_n = 1.16$  MeV, which is larger than the experimental  $S_n = 0.58(9)$  MeV.

Figure 2 shows the GSM results for  $^{20,22}\text{C}$ . For  $^{22}\text{C}$ , only the ground state has been produced in experiment. Our

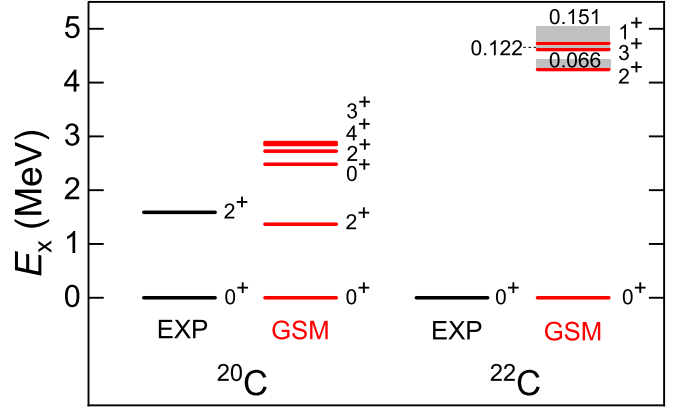


FIG. 2. Similar to Fig. 1 but for  $^{20,22}\text{C}$ . The data are from [33,47].

GSM calculation predicts resonant excited states for  $^{22}\text{C}$ . The calculated first  $2^+$  state in  $^{22}\text{C}$  is at an excitation energy of  $E_x = 4.24$  MeV, which agrees with the RSM [20], CCEI [17], and IMSRG [25] calculations. The large  $2^+$  excitation energy indicates a neutron shell gap at  $N = 16$ . This neutron shell closure also exists in the next even- $Z$  oxygen chain, which has been confirmed experimentally [12]. For  $^{20}\text{C}$ , the GSM calculation presents a low  $2^+$  state at  $E_x = 1.37$  MeV, which agrees with the datum, RSM [20], and CCEI calculations [17]. The low  $2^+$  excitation implies a disappearance of the  $N = 14$  neutron shell closure in the carbon chain. This  $N = 14$  neutron shell closure exists in the oxygen chain. It should be mentioned that in Ref. [25] the Gamow IMSRG gives a lower  $2^+$  state in  $^{22}\text{C}$  between 1.0 and 2.0 MeV depending on interactions used. However, this lower  $2^+$  state is caused by the proton excitation instead of the neutron excitation [25]. Similarly to the RSM [20] and CCEI [17], in the present CD-Bonn GSM calculation we chose  $^{14}\text{C}$  as the inert core, and hence only the neutron excitation is considered.

The GSM calculations shows that the  $^{19}\text{C}$  ground state has a configuration of 85%  $(1s_{1/2})^1 \otimes (0d_{5/2})^4$ , and  $^{22}\text{C}$  has a ground state with 81%  $(1s_{1/2})^2 \otimes (0d_{5/2})^6$ . The  $s$  wave plays an important role in halo structures [8,23].

From the experiment,  $^{21}\text{C}$  is a weakly unbound nucleus with  $T_{1/2} < 30$  ns, and decays by the one-neutron emission [48]. The ground state is assumed to have the spin and parity of  $1/2^+$  [49]. As shown in Fig. 3, the CD-Bonn GSM calculation with the continuum coupling considered reproduces the  $1/2^+$  ground state, while the real-energy SM without the continuum effect considered gives a  $5/2^+$  ground state. The  $1/2^+$  state is dominated by the  $1s_{1/2}$  component, and has a strong coupling to the continuum, which inverts the order between the  $1/2^+$  and  $5/2^+$  levels. However, the GSM calculation gives that the  $1/2^+$  ground state and the first  $5/2^+$  excited state are weakly bound, with the one-neutron separation energies of  $S_n = 0.96$  and  $0.83$  MeV, respectively. The  $3/2^+$ ,  $5/2^+$ , and  $7/2^+$  excited states are calculated to be unbound resonances.

To further understand the neutron shell evolution, we have calculated effective single-particle energies (ESPEs) [50,51], shown in Fig. 4 as a function of the neutron number  $N$ . We see that there is a large  $N = 16$  shell gap between the  $0d_{3/2}$

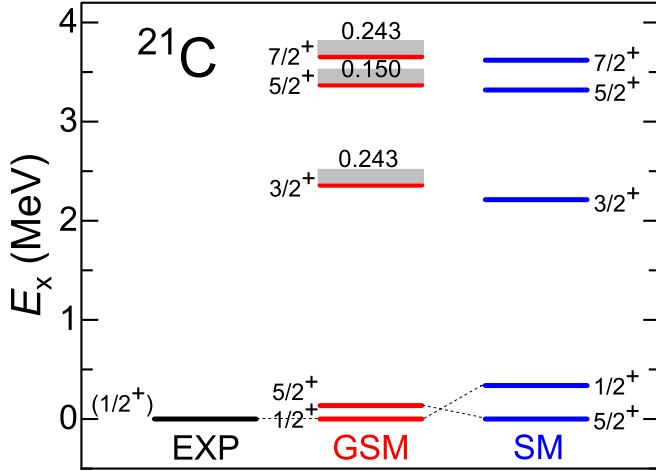


FIG. 3. Similar to Fig. 1 but for  $^{21}\text{C}$ . There is no excited state observed experimentally except the  $(1/2^+)$  ground state [49].

and  $0d_{5/2}/1s_{1/2}$  orbitals. In the neighboring chain of oxygen isotopes, the  $1s_{1/2}$  orbital is located halfway between  $0d_{3/2}$  and  $0d_{5/2}$  [38], which gives neutron shell closures at both  $N = 16$  and 14. The situation is different in the carbon chain where the  $1s_{1/2}$  orbital is lower than the  $0d_{5/2}$  orbital (see Fig. 4), and no shell gap exists between  $0d_{5/2}$  and  $1s_{1/2}$ . This leads to the disappearance of the  $N = 14$  shell closure in the carbon chain and an enhanced  $N = 16$  shell, which is consistent with the experiment [9,10].

Figure 5 gives the ground-state energies of carbon isotopes. The CD-Bonn GSM calculations with the continuum effect considered reproduce reasonably the ground-state energies, and suggest the neutron drip line at  $^{22}\text{C}$ . The calculated ground-state energies of  $^{22-24}\text{C}$  are over-bound by about 4 MeV, compared with the data. It was found that the three-nucleon force (3NF) supplies a significant repulsive contribution to the ground-state energies of the  $N = 16$  oxygen

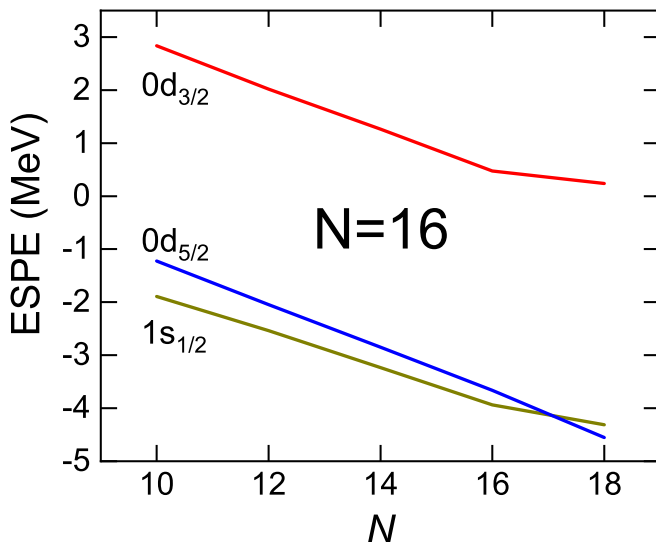


FIG. 4. Calculated effective single-particle energies for the neutron  $1s_{1/2}$ ,  $0d_{5/2}$ ,  $0d_{3/2}$  orbitals.

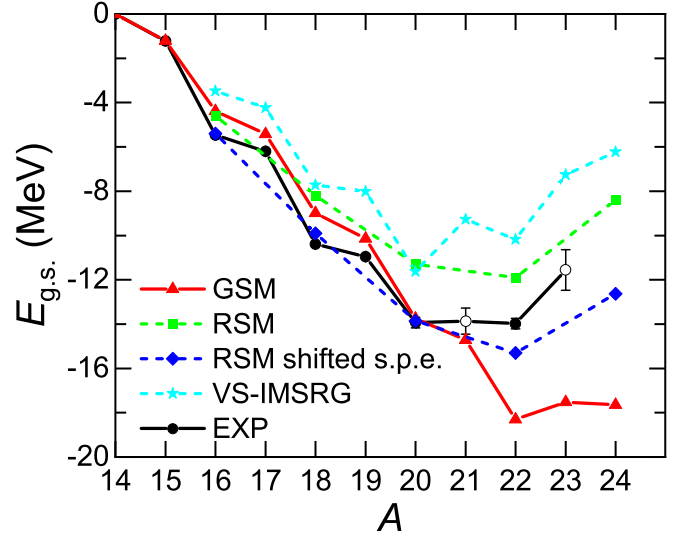


FIG. 5. Experimental [33] and calculated ground-state energies with respect to the  $^{14}\text{C}$  core. The RSM calculations without and with the single-particle energy (s.p.e.) shift are from Ref. [20]. The VS-IMSRG results are from [21]. Data shown with open circles are evaluations taken from [33].

drip line nucleus  $^{24}\text{O}$  and its heavier isotopes [38]. The 3NF repulsive effect should be expected in the  $N = 16$  carbon drip line nucleus  $^{22}\text{C}$  and its heavier isotopes. In Fig. 5, we also show other calculations by the real-energy RSM based on the chiral two-nucleon  $N^3\text{LOW}$  interaction [20] and the real-energy VS-IMSRG using the chiral two- and three-nucleon interactions [21]. In the RSM calculations [20], only even-carbon ground-state energies were given. The RSM single-particle energies were obtained by the so-called  $\hat{S}$  box [20], which was found to underestimate the ground-state energies compared with the data, as shown in Fig. 5. By shifting the single-particle spectrum by  $-427$  keV [20], the RSM calculations are improved significantly. It should be mentioned that in the RSM calculation [20] the  $\hat{Q}$ -box diagrams were calculated up to the third order of the perturbation. In the present GSM calculation, the inclusion of continuum channels makes it infeasible to include third-order  $\hat{Q}$ -box diagrams due to computing power limitations. The third-order  $\hat{Q}$ -box diagrams may capture more dynamic correlations, and produce a visible effect on the energy of the ground state. However, the effect of third-order  $\hat{Q}$ -box diagrams on the excitation energy spectrum is small [28,52].

#### IV. SUMMARY

The descriptions of excitation spectra of neutron-rich carbon isotopes, especially for odd-mass isotopes, remain a theoretical challenge. In this paper, we have investigated the effect from the continuum coupling within the Gamow shell model based on a realistic nuclear force of the CD-Bonn potential.  $^{14}\text{C}$  was chosen as the core of the Gamow shell-model calculation. In this model, the continuum effect is taken into account at the basis level by using the Berggren ensemble in which bound, resonance and scattering continuum states are treated on the same footing. We find that the continuum coupling

plays an important role in reproducing the correct order of the levels in the heaviest odd-mass carbon isotopes of  $^{19,21}\text{C}$ .

However, the level spacing calculated between the first excited state and the ground state is small ( $\lesssim 300$  keV) in  $^{19,21}\text{C}$ . Other factors may also affect the final numerical result, for instance, the three-nucleon force, higher-order diagrams in the  $Q$ -box expansion, and the choice of the cutoff value in the  $V_{\text{low-}k}$  renormalization of the interaction. The neutron-rich carbon isotopes are deformed, for instance, in the mean-field calculation [53]. Though the shell model can treat deformed nuclei through configuration mixing, the calculation truncated with the use of a spherical basis may still miss some non-negligible configurations, and consequently the final numerical results of excitation energies may be affected. In this work, we focus on the effect from the continuum coupling.

The present calculations show that the neutron  $N = 14$  subshell disappears, while the  $N = 16$  shell closure is enhanced, compared with those in the next even- $Z$  chain of oxygen isotopes. The neutron drip line position of the carbon chain, which is at  $^{22}\text{C}$ , is reproduced.

## ACKNOWLEDGMENTS

We thank Nicolas Michel for sharing the GSM code (publicly available [54]) to diagonalize our complex-symmetric GSM Hamiltonian. This work has been supported by the National Key R&D Program of China under Grant No. 2018YFA0404401; the National Natural Science Foundation of China under Grants No. 11835001, No. 11921006, No. 12035001, and No. 12105106; China Postdoctoral Science Foundation under Grants No. BX20200136 and No. 2020M682747; the State Key Laboratory of Nuclear Physics and Technology, Peking University under Grant No. NPT2020KFY13; the Quantum Science Center, a National Quantum Information Science Research Center of the U.S. Department of Energy. Oak Ridge National Laboratory is supported by the Office of Science of the U.S. Department of Energy under Contract No. DE-AC05-00OR22725. We acknowledge the High-Performance Computing Platform of Peking University for providing computational resources.

- 
- [1] A. Ozawa, T. Suzuki, and I. Tanihata, *Nucl. Phys. A* **693**, 32 (2001).
- [2] D. Q. Fang, T. Yamaguchi, T. Zheng, A. Ozawa, M. Chiba, R. Kanungo, T. Kato, K. Morimoto, T. Ohnishi, T. Suda, Y. Yamaguchi, A. Yoshida, K. Yoshida, and I. Tanihata, *Phys. Rev. C* **69**, 034613 (2004).
- [3] R. Kanungo, W. Horiuchi, G. Hagen, G. R. Jansen, P. Navratil, F. Ameil, J. Atkinson, Y. Ayyad, D. Cortina-Gil, I. Dillmann, A. Estradé, A. Evdokimov, F. Farinon, H. Geissel, G. Guastalla, R. Janik, M. Kimura, R. Knöbel, J. Kurcewicz, Y. A. Litvinov *et al.*, *Phys. Rev. Lett.* **117**, 102501 (2016).
- [4] D. Bazin, B. A. Brown, J. Brown, M. Fauerbach, M. Hellström, S. E. Hirzebruch, J. H. Kelley, R. A. Kryger, D. J. Morrissey, R. Pfaff, C. F. Powell, B. M. Sherrill, and M. Thoennessen, *Phys. Rev. Lett.* **74**, 3569 (1995).
- [5] F. M. Marqués, E. Liegard, N. Orr, J. Angélique, L. Axelsson, G. Bizard, W. Catford, N. Clarke, G. Costa, M. Freer, S. Grévy, D. Guillemaud-Mueller, G. Gyapong, F. Hanappe, P. Hansen, B. Heusch, B. Jonson, C. Le Brun, F. Lecomte, F. Lefebvres *et al.*, *Phys. Lett. B* **381**, 407 (1996).
- [6] T. Baumann, M. Borge, H. Geissel, H. Lenske, K. Markenroth, W. Schwab, M. Smedberg, T. Aumann, L. Axelsson, U. Bergmann, D. Cortina-Gil, L. Fraile, M. Hellström, M. Ivanov, N. Iwasa, R. Janik, B. Jonson, G. Münzenberg, F. Nickel, T. Nilsson *et al.*, *Phys. Lett. B* **439**, 256 (1998).
- [7] Y. Togano, T. Nakamura, Y. Kondo, J. Tostevin, A. Saito, J. Gibelin, N. Orr, N. Achouri, T. Aumann, H. Baba, F. Delaunay, P. Doornenbal, N. Fukuda, J. Hwang, N. Inabe, T. Isobe, D. Kameda, D. Kanno, S. Kim, N. Kobayashi *et al.*, *Phys. Lett. B* **761**, 412 (2016).
- [8] K. Tanaka, T. Yamaguchi, T. Suzuki, T. Ohtsubo, M. Fukuda, D. Nishimura, M. Takechi, K. Ogata, A. Ozawa, T. Izumikawa, T. Aiba, N. Aoi, H. Baba, Y. Hashizume, K. Inafuku, N. Iwasa, K. Kobayashi, M. Komuro, Y. Kondo, T. Kubo *et al.*, *Phys. Rev. Lett.* **104**, 062701 (2010).
- [9] M. Stanoiu, D. Sohler, O. Sorlin, F. Azaiez, Z. Dombrádi, B. A. Brown, M. Bellegruic, C. Borcea, C. Bourgeois, Z. Dlouhy, Z. Elekes, Z. Fülöp, S. Grévy, D. Guillemaud-Mueller, F. Ibrahim, A. Kerek, A. Krasznahorkay, M. Lewitowicz, S. M. Lukyanov, S. Mandal *et al.*, *Phys. Rev. C* **78**, 034315 (2008).
- [10] M. J. Strongman, A. Spyrou, C. R. Hoffman, T. Baumann, D. Bazin, J. Brown, P. A. DeYoung, J. E. Finck, N. Frank, S. Mosby, W. F. Rogers, G. F. Peaslee, W. A. Peters, A. Schiller, S. L. Tabor, and M. Thoennessen, *Phys. Rev. C* **80**, 021302(R) (2009).
- [11] M. Stanoiu, F. Azaiez, Z. Dombrádi, O. Sorlin, B. A. Brown, M. Bellegruic, D. Sohler, M. G. Saint Laurent, M. J. Lopez-Jimenez, Y. E. Penionzhkevich, G. Sletten, N. L. Achouri, J. C. Angélique, F. Becker, C. Borcea, C. Bourgeois, A. Bracco, J. M. Daugas, Z. Dlouhy, C. Donzaud *et al.*, *Phys. Rev. C* **69**, 034312 (2004).
- [12] R. Kanungo, C. Nociforo, A. Prochazka, T. Aumann, D. Boutin, D. Cortina-Gil, B. Davids, M. Diakaki, F. Farinon, H. Geissel, R. Gernhäuser, J. Gerl, R. Janik, B. Jonson, B. Kindler, R. Knöbel, R. Krücken, M. Lantz, H. Lenske, Y. Litvinov *et al.*, *Phys. Rev. Lett.* **102**, 152501 (2009).
- [13] Z. Elekes, Z. Dombrádi, R. Kanungo, H. Baba, Z. Fülöp, J. Gibelin, Á. Horváth, E. Ideguchi, Y. Ichikawa, N. Iwasa, H. Iwasaki, S. Kanno, S. Kawai, Y. Kondo, T. Motobayashi, M. Notani, T. Ohnishi, A. Ozawa, H. Sakurai, S. Shimoura *et al.*, *Phys. Lett. B* **614**, 174 (2005).
- [14] Y. Satou, T. Nakamura, N. Fukuda, T. Sugimoto, Y. Kondo, N. Matsui, Y. Hashimoto, T. Nakabayashi, T. Okumura, M. Shinohara, T. Motobayashi, Y. Yanagisawa, N. Aoi, S. Takeuchi, T. Gomi, Y. Togano, S. Kawai, H. Sakurai, H. Ong, T. Onishi *et al.*, *Phys. Lett. B* **660**, 320 (2008).
- [15] Z. Vajta, Z. Dombrádi, Z. Elekes, T. Aiba, N. Aoi, H. Baba, D. Bemmerer, Z. Fülöp, N. Iwasa, A. Kiss, T. Kobayashi, Y. Kondo, T. Motobayashi, T. Nakabayashi, T. Nannichi, H. Sakurai, D. Sohler, S. Takeuchi, K. Tanaka, Y. Togano *et al.*, *Phys. Rev. C* **91**, 064315 (2015).
- [16] J. Hwang, S. Kim, Y. Satou, N. Orr, Y. Kondo, T. Nakamura, J. Gibelin, N. Achouri, T. Aumann, H. Baba, F. Delaunay, P. Doornenbal, N. Fukuda, N. Inabe, T. Isobe, D. Kameda,

- D. Kanno, N. Kobayashi, T. Kobayashi, T. Kubo *et al.*, *Phys. Lett. B* **769**, 503 (2017).
- [17] G. R. Jansen, J. Engel, G. Hagen, P. Navrátil, and A. Signoracci, *Phys. Rev. Lett.* **113**, 142502 (2014).
- [18] C. X. Yuan, T. Suzuki, T. Otsuka, F. R. Xu, and N. Tsunoda, *Phys. Rev. C* **85**, 064324 (2012).
- [19] T. Suzuki and T. Otsuka, *Phys. Rev. C* **78**, 061301(R) (2008).
- [20] L. Coraggio, A. Covello, A. Gargano, and N. Itaco, *Phys. Rev. C* **81**, 064303 (2010).
- [21] S. R. Stroberg, J. D. Holt, A. Schwenk, and J. Simonis, *Phys. Rev. Lett.* **126**, 022501 (2021).
- [22] T. Nakamura, N. Fukuda, T. Kobayashi, N. Aoi, H. Iwasaki, T. Kubo, A. Mengoni, M. Notani, H. Otsu, H. Sakurai, S. Shimoura, T. Teranishi, Y. X. Watanabe, K. Yoneda, and M. Ishihara, *Phys. Rev. Lett.* **83**, 1112 (1999).
- [23] K. Whitmore, D. Smalley, H. Iwasaki, T. Suzuki, V. M. Bader, D. Bazin, J. S. Berryman, B. A. Brown, C. M. Campbell, P. Fallon, A. Gade, C. Langer, A. Lemasson, C. Loelius, A. O. Macchiavelli, C. Morse, T. Otsuka, J. Parker, F. Recchia, S. R. Stroberg *et al.*, *Phys. Rev. C* **91**, 041303(R) (2015).
- [24] D. Smalley, H. Iwasaki, P. Navrátil, R. Roth, J. Langhammer, V. M. Bader, D. Bazin, J. S. Berryman, C. M. Campbell, J. Dohet-Eraly, P. Fallon, A. Gade, C. Langer, A. Lemasson, C. Loelius, A. O. Macchiavelli, C. Morse, J. Parker, S. Quaglioni, F. Recchia *et al.*, *Phys. Rev. C* **92**, 064314 (2015).
- [25] B. S. Hu, Q. Wu, Z. H. Sun, and F. R. Xu, *Phys. Rev. C* **99**, 061302(R) (2019).
- [26] Z. H. Sun, Q. Wu, Z. H. Zhao, B. S. Hu, S. J. Dai, and F. R. Xu, *Phys. Lett. B* **769**, 227 (2017).
- [27] T. Berggren, *Nucl. Phys. A* **109**, 265 (1968).
- [28] B. S. Hu, Q. Wu, J. G. Li, Y. Z. Ma, Z. H. Sun, N. Michel, and F. R. Xu, *Phys. Lett. B* **802**, 135206 (2020).
- [29] R. Machleidt, *Phys. Rev. C* **63**, 024001 (2001).
- [30] J. G. Li, B. S. Hu, Q. Wu, Y. Gao, S. J. Dai, and F. R. Xu, *Phys. Rev. C* **102**, 034302 (2020).
- [31] S. Zhang, Y. Z. Ma, J. G. Li, B. S. Hu, Q. Yuan, Z. H. Cheng, and F. R. Xu, *Phys. Lett. B* **827**, 136958 (2022).
- [32] F. R. Xu, W. Satuła, and R. Wyss, *Nucl. Phys. A* **669**, 119 (2000).
- [33] M. Wang, G. Audi, F. G. Kondev, W. J. Huang, S. Naimi, and X. Xu, *Chin. Phys. C* **41**, 030003 (2017).
- [34] F. Ajzenberg-Selove, *Nucl. Phys. A* **523**, 1 (1991).
- [35] N. Michel, W. Nazarewicz, M. Poszajczak, and T. Vertse, *J. Phys. G: Nucl. Part. Phys.* **36**, 013101 (2009).
- [36] G. Hagen, M. Hjorth-Jensen, and N. Michel, *Phys. Rev. C* **73**, 064307 (2006).
- [37] R. Liotta, E. Maglione, N. Sandulescu, and T. Vertse, *Phys. Lett. B* **367**, 1 (1996).
- [38] Y. Z. Ma, F. R. Xu, L. Coraggio, B. S. Hu, J. G. Li, T. Fukui, L. De Angelis, N. Itaco, and A. Gargano, *Phys. Lett. B* **802**, 135257 (2020).
- [39] Y. Z. Ma, F. R. Xu, N. Michel, S. Zhang, J. G. Li, B. S. Hu, L. Coraggio, N. Itaco, and A. Gargano, *Phys. Lett. B* **808**, 135673 (2020).
- [40] J. G. Li, N. Michel, W. Zuo, and F. R. Xu, *Phys. Rev. C* **103**, 034305 (2021).
- [41] S. Bogner, T. Kuo, and A. Schwenk, *Phys. Rep.* **386**, 1 (2003).
- [42] M. Moshinsky, *Nucl. Phys.* **13**, 104 (1959).
- [43] K. Suzuki, H. Kumagai, R. Okamoto, and M. Matsuzaki, *Phys. Rev. C* **89**, 044003 (2014).
- [44] N. Michel, H. Aktulga, and Y. Jaganathan, *Comput. Phys. Commun.* **247**, 106978 (2020).
- [45] N. Michel and M. Płoszajczak, *Gamow Shell Model: The Unified Theory of Nuclear Structure and Reactions*, Lecture Notes in Physics (Springer, Cham, 2021), Vol. 983
- [46] C. R. Hoffman, B. P. Kay, and J. P. Schiffer, *Phys. Rev. C* **89**, 061305(R) (2014).
- [47] M. Petri, P. Fallon, A. O. Macchiavelli, S. Paschalis, K. Starosta, T. Baugher, D. Bazin, L. Cartegni, R. M. Clark, H. L. Crawford, M. Cromaz, A. Dewald, A. Gade, G. F. Grinyer, S. Gros, M. Hackstein, H. B. Jeppesen, I. Y. Lee, S. McDaniel, D. Miller *et al.*, *Phys. Rev. Lett.* **107**, 102501 (2011).
- [48] <https://www.nndc.bnl.gov/nudat3/>.
- [49] S. Mosby, N. Badger, T. Baumann, D. Bazin, M. Bennett, J. Brown, G. Christian, P. DeYoung, J. Finck, M. Gardner, J. Hinnefeld, E. Hook, E. Lunderberg, B. Luther, D. Meyer, M. Mosby, G. Peaslee, W. Rogers, J. Smith, J. Snyder *et al.*, *Nucl. Phys. A* **909**, 69 (2013).
- [50] Y. Utsuno, T. Otsuka, T. Mizusaki, and M. Honma, *Phys. Rev. C* **60**, 054315 (1999).
- [51] Y. Z. Ma, L. Coraggio, L. De Angelis, T. Fukui, A. Gargano, N. Itaco, and F. R. Xu, *Phys. Rev. C* **100**, 034324 (2019).
- [52] Q. Wu, F. R. Xu, B. S. Hu, and J. G. Li, *J. Phys. G: Nucl. Part. Phys.* **46**, 055104 (2019).
- [53] X. X. Sun, J. Zhao, and S. G. Zhou, *Phys. Lett. B* **785**, 530 (2018).
- [54] <https://github.com/GSMUTNSR>.